Letters

Plasma Science and Technology

Plasma Sci. Technol. **25** (2023) 042001 (4pp) https://doi.org/10.1088/2058-6272/ac9f2d

Letter

Rapid growth of nanostructure on tungsten thin film by exposure to helium plasma

Shuangyuan FENG[1,*], Shin KAJITA[2], Masayuki TOKITANI[1], Daisuke NAGATA[1] and Noriyasu OHNO[3]

[1] National Institute for Fusion Science, National Institutes of Natural Sciences, Toki, Gifu 509-5292, Japan
[2] Graduate School of Frontier Sciences, The University of Tokyo, Kashiwa, Chiba 277-8561, Japan
[3] Graduate School of Engineering, Nagoya University, Nagoya 464-8603, Japan

E-mail: feng.shuangyuan@nifs.ac.jp

Received 16 September 2022, revised 1 November 2022
Accepted for publication 1 November 2022
Published 8 February 2023

Abstract

A fiberform nanostructure was synthesized by exposing high-density helium plasma to a 100 nm thick tungsten thin film in the linear plasma device NAGDIS-II. After helium plasma exposure, the cross-section of samples was observed by a scanning electron microscope, transmission electron microscope, and focused ion beam scanning electron microscope. It is shown that the thickness of the nanostructured layer increases significantly for only a short irradiation time. The optical absorptivity remains high, even though it is exposed to helium plasma for a short time. The usage of the thin film can shorten the processing time for nanostructure growth, which will be beneficial for commercial production.

Keywords: helium plasma, fiberform nanostructure, rapid growth

(Some figures may appear in colour only in the online journal)

1. Introduction

Tungsten (W) is primarily used as a plasma-facing material in fusion reactors [1–4]. When exposed to tokamak-based helium plasma in plasma devices at a laboratory scale, the surface of tungsten will grow fiberform nanostructures (FNs), often referred to as 'fuzz,' under certain conditions [5–11]. The FNs are composed of fibers with diameters of 10–50 nm. There have been many studies on FNs researching detailed mechanisms [6, 10, 12–14], conditions of growth [10, 15], characteristics, and so on. It has been found that favorable formation conditions are surface temperature in the range of 1000–2000 K [15] and incident ion energy greater than 20 eV [10]. Owing to the formation of FN on the material surface, various properties are largely changed in electronics, mechanics, magnetics, optics, etc [16–20]. Although the property changes caused by the formation of FNs have a detrimental effect on fusion reactor performance and operation [21, 22], they have potential applications in many fields and devices, such as solar absorbers [18, 19, 23], photocatalysis [24–26], gas sensors [27], and so on. Petty *et al* first used a magnetron sputtering device to create a tungsten nanostructure [11]. Although the usage of widely available magnetron sputtering expanded the potential application of FNs to various fields, the formation of FNs took a long time, typically more than six hours. The requirement for the formation of FNs is high helium ion fluence, namely, it requires high density and/or a long time. Rapid preparation of FNs is beneficial to better promote the fiberform nanostructure of effective utilization in many industrial fields. Recently, non-uniform isolated nanostructures were formed when He plasma exposure was performed on W thin-film samples in which the film thickness was 100 nm or less [28]. The results suggested that the growth property of FNs on thin films can be quite different from sheet samples, especially when the film thickness is 100 nm or less. In the present article, 100 nm thick tungsten thin films were exposed in a linear plasma device NAGDIS-II [28, 29]. This study compared the growth rates of the FNs on sheet and thin-film samples. We will discuss the difference in the growth process of FNs on the thin-film

* Author to whom any correspondence should be addressed.

Table 1. Irradiation conditions of the thin-film samples in this study.

No.	T_s (K)	Fluence (m^{-2})
W0	1108	6.6×10^{24}
W1	1149	8.7×10^{24}
W2	1169	1.0×10^{25}
W3	1173	1.3×10^{25}
W4	1167	5.2×10^{25}
W5	1090	1.2×10^{26}

sample exposed to He plasma from that on the sheet sample. We will also show the optical absorptivity of nanostructured thin-film samples under low helium fluence and briefly discuss the formation mechanism of the FNs on the thin-film sample.

2. Experiments

The substrate used in this experiment was $10 \times 10\,mm^2$ quartz glass (Labo-USQ, 1 mm thickness). 100 nm thick tungsten thin films were deposited on substrates by a radio frequency (RF) magnetron sputtering apparatus. After deposition, the linear plasma irradiation device NAGDIS-II was used to obtain fiberform nanostructure in the experiment. High-density helium plasma could be formed by a direct current arc discharge using a LaB_6 cathode. A single probe was used to measure the electron density ($\sim 10^{18}$–10^{19} m^{-3}) and temperature (~5 eV). A radiation pyrometer was applied to measure the surface temperature after starting the plasma irradiation. Negative bias was applied to the tungsten thin-film samples. The negative bias of all samples was −90 V. In this study, −90 V was chosen to obtain high incident ion energy and easier generation of fiberform nanostructures. The irradiation conditions of different samples are summarized in table 1. The samples were numbered from W0 to W5, as shown in table 1. In this study, the He fluence was altered from 6.6×10^{24} (W0) to 1.2×10^{26} (W5) m^{-2} at the surface temperature of 1090–1173 K. To evaluate the effects of helium ion fluence on the thickness of the nanostructured layer, the tungsten thin-film samples were irradiated for various helium ion fluences. The surface and cross-sectional morphology observations were processed by a scanning electron microscope (SEM), a focused ion beam scanning electron microscope (FIB-SEM, nanoDUE'T NB5000, Hitachi High-Technologies Corp.), and a transmission electron microscope (TEM). The optical reflectivity was carried out using a UV-Vis spectrophotometer (UV-2600). The transmissivity was measured using a UV-VIS-NIR spectrophotometer (UV-3600i Plus).

3. Results and discussion

Figures 1(a) and (b) show the surface and cross-sectional micrographs of the W1 sample, respectively, which was exposed to the helium plasma with a helium fluence of 8.7×10^{24} m^{-2}. The island-shaped nanostructures were

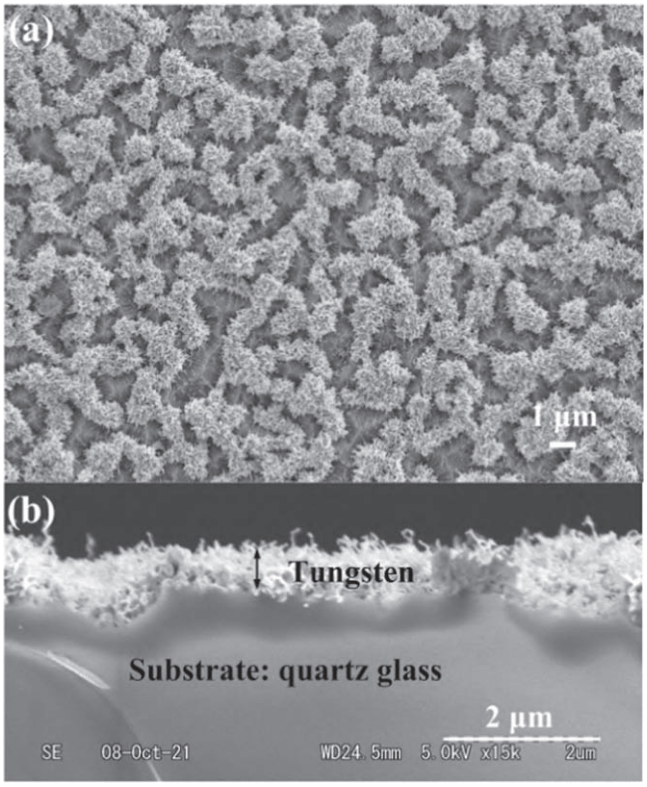

Figure 1. FE-SEM surface and SEM cross-sectional images of helium-irradiated tungsten thin film with a helium fluence of 8.7×10^{24} m^{-2}.

formed on the surface, and the thickness of the layer was approximately 550 nm. In figure 1(b), the island structure cannot be clearly identified because the sample was not cut to a thin film, using a focused ion beam (FIB). Figures 2(a)–(c) show TEM micrographs of the W2 sample. The TEM sample was prepared with FIB milling after a carbon coating. The sample was prepared in the form of a thin film, so the individual island-shaped nanostructures can be clearly seen. Some self-assembling processes should exist behind the formation of such island structures; the mechanism has yet to be understood. One of the possible causes of the island-shaped nanostructure is that due to the difference in the thermal expansion coefficient, the nanostructure cannot follow the thermal expansion of the SiO_2 substrate.

The part without nanostructures (the red circle part) in figure 2(a) corresponds to the middle of the island-shaped nanostructures in figure 1(a). It can be seen from figures 2(b) and (c) that the thin film became fibers almost totally without remaining in the bulk layer, and it seems that fibers also grow downward. This is probably because of the swelling process due to the growth of He bubbles, as was discussed in [30]. Because the thickness of W thin film is just 100 nm, the implanted He atoms probably cannot easily diffuse to a deeper region due to the barrier between the SiO_2 substrates, as no He bubbles can be identified on the SiO_2 substrate beneath the fuzz layer. Due to limited diffusion in the depth direction, the He density in the top layer can be higher than those in sheet sample cases. In addition, in the region where W atoms were removed and He ions could reach the SiO_2

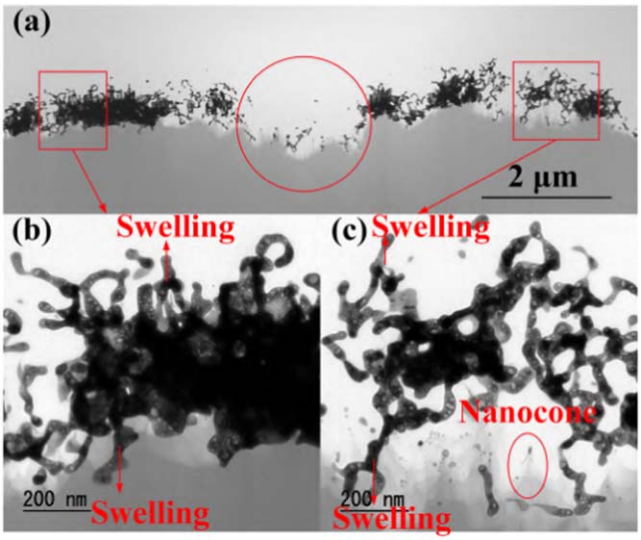

Figure 2. TEM cross-sectional images ((a)–(c)) of helium-irradiated tungsten thin film with a helium fluence of 1.0×10^{25} m^{-2}, (b) and (c) are partial enlarged images in (a), respectively.

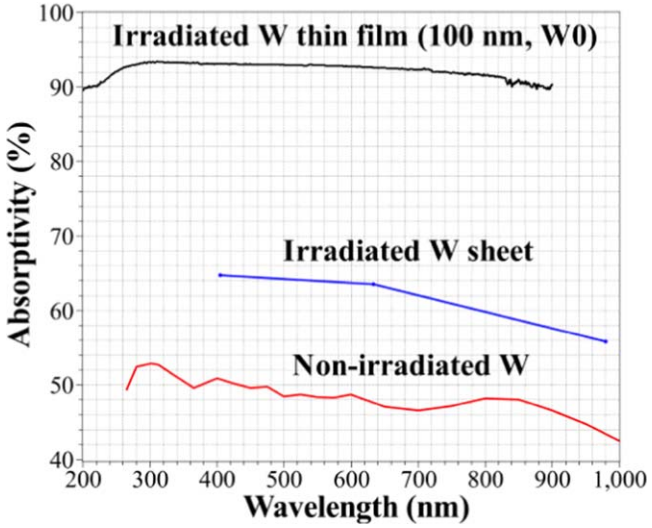

Figure 3. (Black line) Wavelength dependence of the optical absorptivity of the helium-irradiated W0, derived from the specular reflection spectrum and transmissivity. The red curve is the wavelength dependence of the optical absorptivity of non-irradiated W. The blue line with markers is the wavelength dependence of the absorptivity of the irradiated W sheet sample with the helium fluence from [19].

substrate, nanocones were identified on the SiO_2 surface, similar to Si nanocones formed by He ion irradiation [31]. Because a darker droplet can be found on the tip of the nanocone, which is marked with a red circle in figure 2(c), the formation mechanism is the same as that on the Si substrate, on which sputtering played a major role for the nanocone formation.

Figure 3 shows the wavelength dependence of optical absorptivity, derived from the specular reflection spectrum and transmission spectrum, for W0. The helium fluence is 6.6×10^{24} m^{-2}. The red and blue lines with markers are the

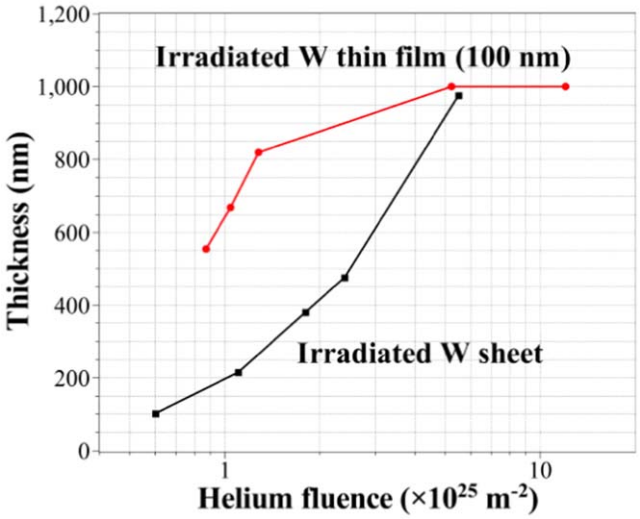

Figure 4. Thickness of the nanostructured layer versus the helium fluence (nanostructured thin-film samples: red/circle, using the data from W1 to W5, nanostructured sheet samples: black/rectangle). The data of the nanostructured sheet samples are from [32].

wavelength dependence of the absorptivity of the non-irradiated W and irradiated W sheet sample with a helium fluence of 4.6×10^{24} m^{-2}, respectively. The absorptivity reaches 90% in the visible region, even though the irradiation time of W0 is very short (180 s). The helium fluence of nanostructured thin-film samples is much lower, as compared to that of nanostructured sheet samples, in order to achieve the same optical absorptivity. The absorptivity of the nanostructured sheet sample under a similar helium fluence is about 60% [19].

Figure 4 plots the thickness of the nanostructured layer grown on thin film and sheet samples as a function of the helium fluence. The helium fluence of W2 is 1.0×10^{25} m^{-2}, which is slightly lower than that of W3 (1.3×10^{25} m^{-2}). As the helium fluence increased slightly, the nanostructured layer became thicker by comparing W3 (~819 nm) to W2 (~668 nm). The nanostructured layer thickness of W3 was approximately 1.2 times that of W2. As compared to the increase in the helium fluence, the thickness of the nanostructured layer did not change significantly from W3 (~819 nm) and W4 (~1000 nm), though the fluence increased more than four times. The helium fluence of W4 and W5 are 5.2×10^{25} and 1.2×10^{26} m^{-2}, respectively. The thickness of the nanostructured layer did not increase with the helium fluence, comparing W4 and W5 (~1000 nm). The results indicate that as the helium fluence increases, the nanostructured layer thickness increases and finally approaches a saturated value (~1 μm). As can be seen from figure 4, the thickness of the nanostructured layer on thin-film samples is thicker than that on the sheet samples when the helium fluence is low, say lower than $\sim 5 \times 10^{24}$ m^{-2}. Petty and his colleagues collected data from various devices and concluded that He fluence is a sole key factor to determining the fuzzy layer thickness. In other words, the fuzzy thickness can be determined by the He fluence when other competing processes such as annealing [33] and sputtering [34] do not work.

That is, the growth process is determined by some diffusion-limited process, though the exact process has yet to be identified. Numerous studies have investigated the growth model of nanostructures under high fluence, and it follows a square root of fluence ($\Phi^{1/2}$) fit [6]. Petty investigated the growth model under low fluence and found it also followed a $\Phi^{1/2}$ fit. It is reported by Baldwin *et al* that there was an incubation time necessary for fuzz growth [35]. It is more convenient to discuss using fluence rather than time so as to be able to compare all devices [36]. Researchers have been able to use incubation fluence for experiments with low fluxes and long exposure times. However, in the case of large flux and an extremely short irradiation time, such a time is not enough for fuzz growth. This implies that some inherent incubation time is necessary for fuzz to grow. Regarding the results of figure 4, it seems that the present thin-film samples in this study under low fluence have a short incubation time. Although an enhanced growth process has recently been identified with auxiliary W deposition [37], the enhanced growth identified in this work is an interesting process because it violates the diffusion-limited process, especially when the He fluence is low ($<10^{25}$ m^{-2}). One of the key factors that is not consistent with the square root of fluence, as Petty stated, is likely to be the increase in the density of He atoms on the top layer because of the limited diffusion toward the deeper region. One possible reason is the thermal deformation of the SiO_2 substrate that formed the island structure. As can be seen from figure 2(a), the deformation of the SiO_2 substrate has already occurred and there is little tungsten thin film in the concave part of the substrate. The convex part of the substrate was far more likely to be entered than the concave part. The island structure can be formed more easily. In the future, it will be of interest to investigate the amount of He atoms on the thin layer by using thermal desorption spectroscopy. One of the disadvantages of this work is the non-uniformity of the fuzzy layer. It is of importance to investigate this non-uniformity in lower fluence.

4. Summary

In conclusion, in this study, tungsten thin-film samples were exposed to helium plasma and it was found that as the helium fluence increased, the nanostructured thickness grew rapidly. The optical absorptivity of W0 at low helium fluence is very high, up to about 90%, which will provide the foundation for its optical application. As mentioned earlier, the preparation time of existing preparation methods for generating fiberform nanostructures is very long [11]. Irradiation with thin-film samples brings many advantages, such as a short preparation time and high optical absorptivity, which may make the application scope for obvious expansion. This synthesizes the merits of high optical absorptivity and short formation time, and offers a new effective option for optical application.

ORCID iDs

Shuangyuan FENG https://orcid.org/0000-0001-8616-6041

References

[1] Ueda Y *et al* 2014 *Fusion Eng. Des.* **89** 901
[2] Neu R *et al* 2016 *Fusion Eng. Des.* **109–111** 1046
[3] Wurster S *et al* 2013 *J. Nucl. Mater.* **442** S181
[4] Dasgupta D *et al* 2019 *Nucl. Fusion* **59** 086057
[5] Takamura S *et al* 2006 *Plasma Fusion Res.* **1** 051
[6] Baldwin M J and Doerner R P 2008 *Nucl. Fusion* **48** 035001
[7] Wang K *et al* 2017 *Sci. Rep.* **7** 42315
[8] Yang Q *et al* 2015 *Sci. Rep.* **5** 10959
[9] Wright G M *et al* 2013 *J. Nucl. Mater* **438** S84
[10] Kajita S *et al* 2009 *Nucl. Fusion* **49** 095005
[11] Petty T J and Bradley J W 2014 *J. Nucl. Mater.* **453** 320
[12] Krasheninnikov S I *et al* 2011 *Phys. Scr.* **T145** 014040
[13] Martynenko Y V and Nagel M Y 2012 *Plasma Phys. Rep.* **38** 996
[14] Lasa A, Tähtinen S K and Nordlund K 2014 *Europhy. Lett.* **105** 25002
[15] Sakaguchi W *et al* 2010 *Plasma Fusion Res.* **5** S1023
[16] Nishijima D *et al* 2011 *J. Nucl. Mater* **415** S96
[17] Patino M, Raitses Y and Wirz R 2016 *Appl. Phys. Lett.* **109** 201602
[18] Kajita S *et al* 2010 *Appl. Phys. Express* **3** 085204
[19] Kajita S *et al* 2011 *Jpn. J. Appl. Phys.* **50** 08JG01
[20] Kajita S *et al* 2016 *Results Phys.* **6** 877
[21] Wirth B D *et al* 2015 *J. Nucl. Mater.* **463** 30
[22] Kajita S *et al* 2014 *Nucl. Fusion* **54** 033005
[23] Tripathi J K, Novakowski T J and Hassanein A 2015 *Appl. Surf. Sci.* **353** 1070
[24] Kajita S *et al* 2013 *J. Appl. Phys.* **113** 134301
[25] de Respinis M *et al* 2013 *ACS Appl. Mater. Interfaces* **5** 7621
[26] Feng S Y *et al* 2022 *Appl. Surf. Sci.* **580** 151979
[27] Ibano K *et al* 2018 *Jpn. J. Appl. Phys.* **57** 040316
[28] Feng S Y *et al* 2020 *Mater. Res. Express* **7** 075007
[29] Ohno N *et al* 2001 *Nucl. Fusion* **41** 1055
[30] Kajita S *et al* 2015 *New J. Phys.* **17** 043038
[31] Takamura S *et al* 2019 *Appl. Surf. Sci.* **487** 755
[32] Kajita S *et al* 2011 *J. Nucl. Mater.* **418** 152
[33] De Temmerman G, Doerner R P and Pitts R A 2019 *Nucl. Mater. Energy* **19** 255
[34] Noiri Y, Kajita S and Ohno N 2015 *J. Nucl. Mater.* **463** 285
[35] Baldwin M J *et al* 2009 *J. Nucl. Mater.* **390–391** 886
[36] Petty T J *et al* 2015 *Nucl. Fusion* **55** 093033
[37] Kajita S *et al* 2018 *Sci. Rep.* **8** 56